Estimation of Regional Evapotranspiration Based on the Decouple Model and Remote Sensing Information –a Case Study in Beijing City and Nearby Region

Su-Chuang Di, Zhao-Liang Li, Yanmin Ren, Meng Liu, Ya-Zhen Jiang, Fan-Dong Zheng, Xue-Min Li, Yan-Bing Qi, Hong-Lu Liu, Ronglin Tang

Estimation of Regional Evapotranspiration Based on the Decouple Model and Remote Sensing Information ——a Case Study in Beijing City and Nearby Region

Su-chuang Di [1,2], Zhao-liang Li[3,4,5*], Yanmin Ren[6], Meng Liu[4], Ya-zhen Jiang[3], Fan-dong Zheng[1,2], Xue-min Li [1,2], Yan-bing Qi[1,2], Hong-lu Liu [1,2], Ronglin Tang[3]

1. Beijing Water Science and Technology Institute, Beijing, 100048;
2. Bejing Engineering Research Center for Non-conventional Water Resources Utilization and Water Saving, Beijng, 100048;
3. Institute of Geographic Sciences and Natural Resources Research, Chinese Academy of Sciences, Beijing, 100101;
4. Key Laboratory of Agri-informatics, Ministry of Agriculture Institute of Agricultural Resources and Regional Planning, Chinese Academy of Agricultural Sciences, Beijing, 100081;
5. ICube, UdS, CNRS; 300 Bld Sebastien Brant, CS 10413, 67412 Illkirch, France;
6. Research Center of Information Technology, Beijing Academy of Agriculture and Forestry Sciences, Beijing 100097, China;

Abstract

Evapotranspiration (ET) is an important component of surface energy balance and a key process of hydrological cycle. Continuous and accurate estimation of regional ET is meaningful for water management, agricultural production, and climate change adaptation. Remote Sensing (RS) technique is of important meaning for estimating ET on regional scale. However, there are some problems in the ET estimation model based on RS such as: (1) Surface resistance and aerodynamic resistance which are necessary in energy balance method are not easy to be estimated accurately, (2) Advective energy, which is an important driver of ET in heterogeneous regions, is not accounted for. In this study, a new method is developed to integrate the RS information and meteorological data based on the decouple model which is deduced from Penman-Monteith (PM) model. Firstly, a parameterization method for decoupling factor (Ω) which is key parameter in the decouple model and could reflect the coupling relationship between the land surface and atmosphere systems is introduced. Subsequently, the decouple model is applied to inverse regional ET in Beijing City and nearby region, from 1st, May, 2013 to 31th, October, 2020. Thirdly, the inversed daily ET values are evaluated based on the measured data at Huailai station and in Badaling

Forest Farm. The results show that the changing trend of estimated ET and measured ET are basically the similar.The mean value of the daily estimated ET is 1.40 mm d^{-1} and the mean value of the daily measured ET is 1.52 mm d^{-1}. The bias value is -0.12 mm d^{-1}, the RSME value is 0.66 mm d^{-1}, and the correlation coefficient is 0.52 . Finally, the spatiotemporal trend of water consumption in study area is analyzed based on the ET estimation results. The month with the largest water consumption in 2013 is July with the quantity of 0.92 billion m^3, accounting for about 22% of the regional total water consumption in growing season. The regions with high ET values agree well with the regions of high soil moisture and high air humidity as well as high biomass. These results suggest that the decouple model is with great potential to generate regional daily ET products and to support irrigation management.

Key Words: Evapotranspiration (ET), Decouple model, Surface resistance, Water Consumption

1. Introduction

Evapotranspiration (ET) is an important component of surface energy balance and a key process of hydrological cycle (Zhang et al. 2016; Zhao et al. 2013; Jung et al. 2010). Continuous and accurate estimations of regional ET are meaningful for water management, agricultural production, and climate change adaptation (Granata 2019; Kool et al. 2014). Remote Sensing (RS) technique is of important meaning for estimating ET on regional scale (Kool et al. 2014). In the past 40 years, the use of remote sensing technology to carry out regional ET estimation research has achieved fruitful results, forming a series of theories and methods (Li et al. 2009), which can be roughly divided into: 1) empirical regression models enable direct calculation of ET by establishing simple empirical equations through statistical analysis of in-situ and remote sensing observations (Wang et al. 2007; Jackson et al. 1977), e.g. Wang et al. (2007) directly established the relationship between net radiation, land surface temperature (or air temperature) and vegetation index and evapotranspiration to achieve the estimation of daily average ET; 2) energy balance models, based on the energy balance residual method to calculate ET, are represented by SEBI (Menenti and

Choudhury 1993), SEBAL (Bastiaanssen 2000; Tang et al. 2013), SEBS (Su 2002), N95 (Kustas and Humes 1995), etc.; 3) vegetation index-surface temperature space models, based on spatial background information, use remote sensing data to identify the boundary conditions in the evaporation process by some physical or empirical methods to calculate ET (Tang et al. 2010; Long et al. 2013; Ronglin. Tang and Li 2017); 4) Penman-Monteith (PM) models, based on Penman equation, use surface resistance to calculate ET (Penman 1948; Monteith J 1965); 5) data assimilation models, represented by Variational Assimilation (Caparrini et al. 2004) and Ensemble Kalman Filter (Reichle et al. 2002), are used to generate ET products with high temporal resolution over long time series by fusing data from multiple sources. However, there are some problems in the ET estimation model based on RS such as: (1) Surface temperature parameters cannot be obtained from thermal-infrared remote-sensing data under cloudy conditions (Crosson et al. 2012; Duan et al. 2017; Ma et al. 2022; Wu et al. 2022), (2) Advective energy, which is an important driver of ET in heterogeneous regions, is not accounted for (Li et al. 2009), (3) Surface resistance and aerodynamic resistance which are necessary in energy balance method are not easy to estimated accurately (Tian et al. 2011; Kang et al. 2019; Yuan et al. 2021).

Meteorological data or re-analysis of data has been used to make up for the shortcomings of RS data, because it has good continuity and it can provide the information that cannot be directly and effectively obtained by remote sensing technology, such as air temperature, saturated water vapor pressure difference, etc. How to integrate the parameters of remote sensing inversion with meteorological data or re-analysis data in order to accurately and continuously estimate surface evapotranspiration at the regional scale is an important field in current evapotranspiration researches (Wang and Dickinson 2012).

The decouple model which is deduced from Penman-Monteith (PM) model, using a decoupling factor of Ω to intuitively and quantitatively represent coupling relationship between land surface and atmosphere systems or to weigh the dominance of wind speed, vegetation stomata, etc. driving the continuation of ET process, could partially solve these problems by combining the remote sensing information and meteorological data

or reanalysis data (Mu et al. 2007; Ramoelo et al. 2014; Di et al. 2015; Mu et al. 2011). Further, Ω is the combination of surface resistance and aerodynamic resistance, which can partially compensate for errors in resistance calculations. Besides, the decouple model, on the one hand, takes into account more comprehensive ET factors by adding soil moisture, vegetation conditions and atmosphere, to obtain better estimation accuracy; on the other hand, the decouple model is more applicable as it can estimate ET in both clear and cloudy days. However, Ω is influenced by these factors such as land surface soil moisture, vegetation condition, wind speed, air temperature, and air humidity, therefore there are no general methods to parameterize Ω on regional scale and the Decouple model is rarely used to estimate the regional ET. In this study, we present a parameterization method for Ω on regional scale, and the decouple model is applied to inverse regional ET in Beijing City and nearby region as a case study to identify the spatiotemporal trend of water consumption in study area as well as to support irrigation management.

2. Study area and data

2.1 Study area

The study area locates in north region of China with a total area of 40910 km^2 (Latitude: 39.305 °N ~ 41.140 °N，Longitude: 115.238 °E ~ 117.594 °E), and it covers whole region of Beijing City and part of Tianjin City and Hebei Province.

The northwest part is mountainous area with the elevation between 100 m and 2411 m and the land covers include forest, shrub, grassland. However, the southeast part is mainly plain area with the elevation below 100 m and the land covers include arable land, construction land.

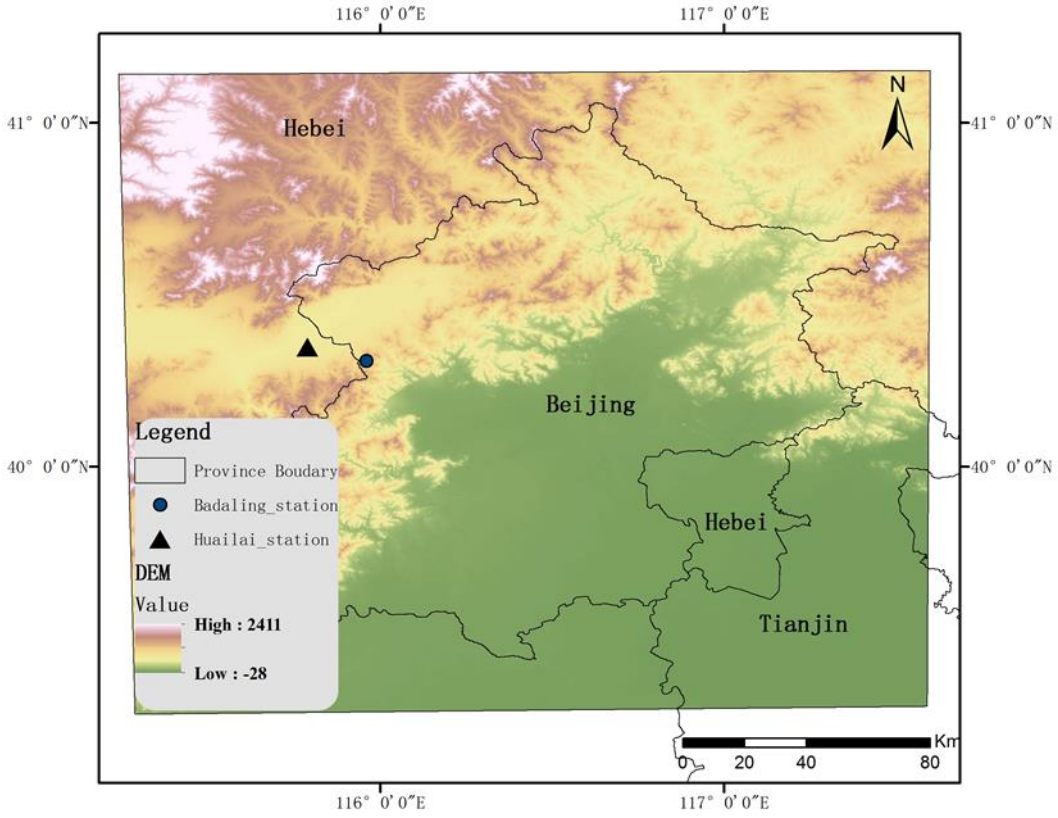

Figure 1. Study region location and elevation information

2.2 Data

The inputs datasets for the decouple model include three categories: (1) remote sensing products, such as vegetation indices, reflectance which are downloaded from MODIS products website with spatial resolution of 500 m, (2) reanalysis datasets, such as solar radiances, air temperature, air humidity, atmospheric pressure, wind speed, soil moisture which are downloaded from China Metrological Administration Land Data Assimilation System (CLDAS) with spatial resolution of 0.0625 °, (3) basic geography information such as vegetation type map, soil texture map which are provided by the Institute of Geographic Sciences and Natural Resources Research, Chinese Academy of Sciences with the scale of 1:4000000.

To validate the ET estimation results, the measured fluxes data and meteorological data at Huailai station (40.3491 °N, 115.7880 °E, 480 m) from 2013 to 2020 is provided by the Cold and Arid Region Science Data Center, China. The automatic weather station at Huailai station is equipped on 10 m tower and provides meteorological data such as air temperature, relative humidity, and wind speed. The eddy-covariance

systems at Huailai station with frequency of 10 Hz and height of 5 m provide flux data such as sensible heat fluxes, latent heat fluxes, etc., where the measured ET values at the Huailai station are derived from latent heat flux. Besides, the meteorological data measured from 6th, May to 6th, October, 2013 in Badaling Forest Farm (40.2833 °N, 115.9167 °E, 674m) is applied to estimate the reference ET (ET_0) of the crop, and the trend of the reference ET is compared with that of ET estimation results. Besides, ET_0 is translated into ET using the PM equation combined with crop coefficients and is compared to daily inversed ET.

3. Methodologies

3.1 Decouple model introduction

Based on PM model, McNaughton and Jarvis (1983) developed the decouple model to describe the interrelation between vegetation and atmosphere system and to study their contributions to the ET. The driving forces for ET are grouped as 2categories: one is the direct solar radiation and the other is the sensible heat absorbed from nearby air. The ratio between the two forces is influenced by the coupling relationship between the land surface and atmosphere systems and it was described as a decoupling coefficient of Ω (Tang and Li 2017). Ω is the combination of surface resistance and aerodynamic resistance, and is used as a key parameter to characterize the degree of coupling between atmospheric and surface systems, which is also closely related to soil moisture (Rana et al. 1997), vegetation types (Goldberg and Bernhofer 2001), surface resistance, and wind speed (Goldberg and Bernhofer 2001), etc..

$$ET = ET_{rad} + ET_{aero} = \Omega E_{eq} + (1-\Omega)E_{im} \quad (3\text{-}1)$$

$$\Omega = \frac{\Delta/\gamma + 1}{\Delta/\gamma + 1 + r_s/r_a} \quad (3\text{-}2)$$

$$E_{eq} = \frac{\Delta}{\Delta+\gamma}\frac{(R_{nd} - G_d)}{\lambda} \quad (3\text{-}3)$$

$$E_{im} = \frac{\rho \cdot c_p \cdot VPD}{\lambda \cdot \gamma \cdot r_s} \quad (3\text{-}4)$$

where ET_{rad} is the radiation component, mm d^{-1}. ET_{aero} is the aerodynamics component, mm d^{-1}. E_{eq} is the equilibrium ET, mm d^{-1}. E_{im} is the imposed ET, mm d^{-1}. λ is the latent

heat of *ET*, MJ kg^{-1}. R_{nd} is the daily net radiation, MJ m^{-2} d^{-1}. G_d *is* the daily soil heat flux, MJ m^{-2} d^{-1} Ω is the decoupling coefficient, (-). Δ represents the slope of the saturation vapor pressure temperature relationship, kPa ˚C^{-1}. γ is the psychrometric constant, kPa ˚C^{-1}. *VPD* is the vapor press deficit, kPa. r_s and r_a are the surface and aerodynamic resistances, s m^{-1}. ρ is the mean air density at constant pressure, kg m^{-3}.c_p is the specific heat of the air, MJ kg^{-1} ℃ $^{-1}$.

3.2 Ω parameterization method

According to the princle of decouple model and the land surface heterogeneity, Ω could be decomposed into three parts: the first part is f_{wet} which repressets the coupling relationship betweet the wet surface and the atomsphere, the second part is Ω_v which repressets the coupling relationship betweet the vegetaton system and the atomsphere, the third part is Ω_s which repressets the coupling relationship betweet the soil system and the atomsphere.

$$\Omega=f_{wet}+(1-f_{wet})\cdot f_c\cdot\Omega_v+(1-f_{wet})\cdot(1-f_c)\cdot\Omega_s \quad (3\text{-}5)$$

$$f_{wet}=\begin{cases}0 & RH<70\% \\ (RH)^4 & RH\geq 70\%\end{cases} \quad (3\text{-}6)$$

$$\Omega_v=\frac{\Delta+\gamma}{\Delta+\gamma\left(1+\frac{r_c}{r_a}\right)} \quad (3\text{-}7)$$

$$\Omega_s=\frac{\Delta+\gamma}{\Delta+\gamma\left(1+\frac{r_{ss}}{r_a}\right)} \quad (3\text{-}8)$$

$$r_{ss}=\exp(n-m\times R_{sm}) \quad (3\text{-}9)$$

$$r^*=\frac{\Delta+\gamma}{\Delta}\cdot\frac{\rho c_p VPD}{\gamma(R_n-G)} \quad (3\text{-}10)$$

$$\frac{r_c}{r_a}=a\cdot\frac{r^*}{r_a}+b \quad (3\text{-}11)$$

$$r_a=\frac{\ln\left(\frac{z_m-d}{z_{om}}\right)\ln\left(\frac{z_h-d}{z_{oh}}\right)}{k^2u_m} \quad (3\text{-}12)$$

where f_c is the vegetation fraction, (-). *RH* is the air relative humidity, (-). r_c is the company resistance, s m^{-1}. r_{ss} is the soil surface resistance, s m^{-1}. R_{sm} is the surface soil moisture, (-). r^* *is* critical resistance, s m^{-1}. *m* and *n* are empirical constant according to soil texture (Di et al. 2015). *a* and *b* are regression coefficients which depend on soil

adjusted vegetation index (SAVI) time series information (Fisher et al. 2008; Kustas et al. 1998). z_m is the height of wind measurement, m. z_h is the height of humidity measurement, m. d is the zero plane displacement height, m. z_{om} is the roughness length governing momentum transfer, m. z_{oh} is the roughness length governing transfer of heat and vapour, m. k is the von Karman's constant, 0.41 (-). u_m is the wind speed at height z_m, m s^{-1}. d， z_{om} and z_{oh} are highly correlated with the vegetation height h_v, and they are estimated according to empirical method (Allen et al., 1998).

The CWSI (Crop Water Stress Index) method was proposed by Jackson et al. (1988) and is calculated as：

$$CWSI = \frac{(T_s - T_a) - (T_s - T_a)_{min}}{(T_s - T_a)_{max} - (T_s - T_a)_{min}} \quad (3\text{-}12)$$

When the surface is fully supplied with water and the surface resistance is minimal, the corresponding evaporation is the maximum potential ET (ET_P); when the moisture is restricted, the surface resistance is r_s and the corresponding actual ET is ET_A. Assuming all other conditions are the same, the following relationship exists between potential evaporation and actual evaporation:

$$\frac{ET_A}{ET_P} = \frac{\Delta + \gamma^*}{\Delta + \gamma(1 + r_s / r_a)} \quad (3\text{-}13)$$

$$\gamma^* = \gamma(1 + r_{s,min}/r_a) \quad (3\text{-}14)$$

Where, $r_{s,min}$, the minimum of surface resistance, s m^{-1}， with the value of 0.

The equation 3-13 is consistent with the Ω expression (equation 3-2), thus yields:

$$\frac{ET_A}{ET_P} = \Omega \quad (3\text{-}15)$$

Meanwhile, Yang (2014) proposed the following relationship between CWSI, actual ET and maximum potential ET:

$$1 - CWSI = \frac{ET_A}{ET_p} \quad (3\text{-}16)$$

Thus, regional ET is estimated by using regional potential evapotranspiration ET_p and Ω parameter (Boegh et al. 2002; Rana et al. 1997).

$$ET_A/ET_P = \Omega = 1\text{-}CWSI \quad (3\text{-}17)$$

3.3 Regional ET estimation procedures

Firstly, parameter *a* and *b* are inferred by SAVI time series datasets which are inferred from MODIS reflectance products in vegetation growing season which is from 1st, May, 2013 to 31th, October, 2020. Secondly, $r^* r_a^{-1}$ is estimated by using reanalysis datasets. Secondly, $r_c r_a^{-1}$ and Ω_v is estimated by combining *a*, *b* and $r^* r_a^{-1}$. Thirdly, R_{sm} is estimated based on the soil texture, soil moisture reanalysis datasets (Di et al. 2015). Fourthly, r_{ss} and Ω_s are estimated by using R_{sm}.and f_{wet} is estimated by using *RH*. Fifthly, Ω is estimated by using $f_{wet,}$ Ω_s and Ω_v. Further, regional potential evapotranspiration ET_p is estimated by using reanalysis datasets and MODIS imagines. Finally, ET_A is estimated by using ET_P and Ω.

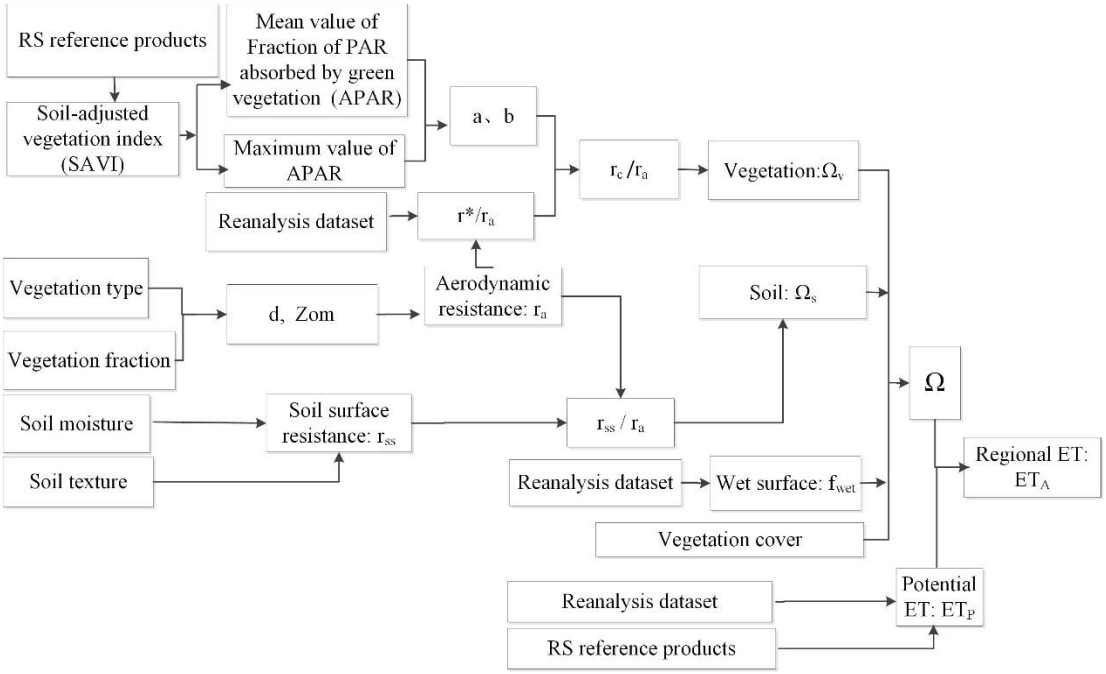

Figure 2. Regional ET inversion procedure using the decouple model

4. Results and discussion

4.1 Regional ET calculation results and precision evaluation

4.1.1 Regional ET calculation results on a typical day

The date of 1st, September, 2013 is seleccted to describes the Decoule model calculation procedure and intermediate results as a typical day. The esimated Ω_v ranges from 0.20 to 0.99 with the mean value of 0.26 and the esimated Ω_s ranges from 0.16 to 0.95 with the mean value of 0.39. Esimated f_{wet} ranges from 0 to 0.32 with the mean value of 0.04 and the region with high f_{wet} values distribute in the northeast region of the study area. The esimated f_c ranges from 0.01 to 0.99 with the mean value of 0.66.

Based on these results, reginal Ω is parameterized, and it ranges from 0.22 to 0.62 with the mean value of 0.31 and the high values distribute in the north, east and central region of the study area, as shown in Fig.3 (the null value region is build-up area and water body).

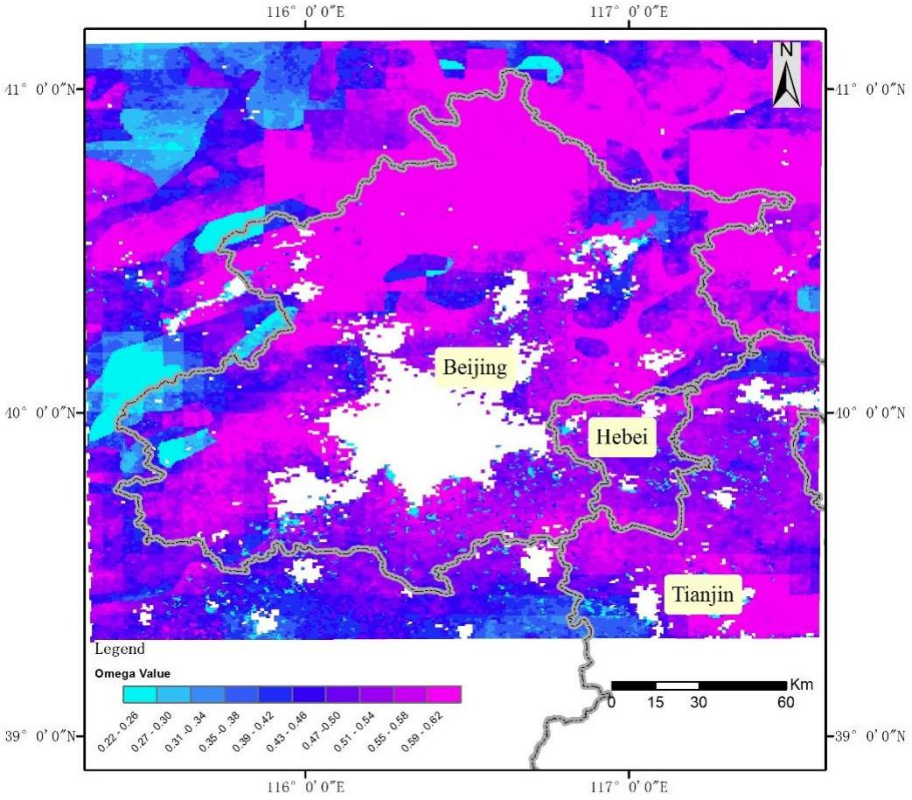

Figure 3.a. Estimated Ω spatial distribution (20130901)

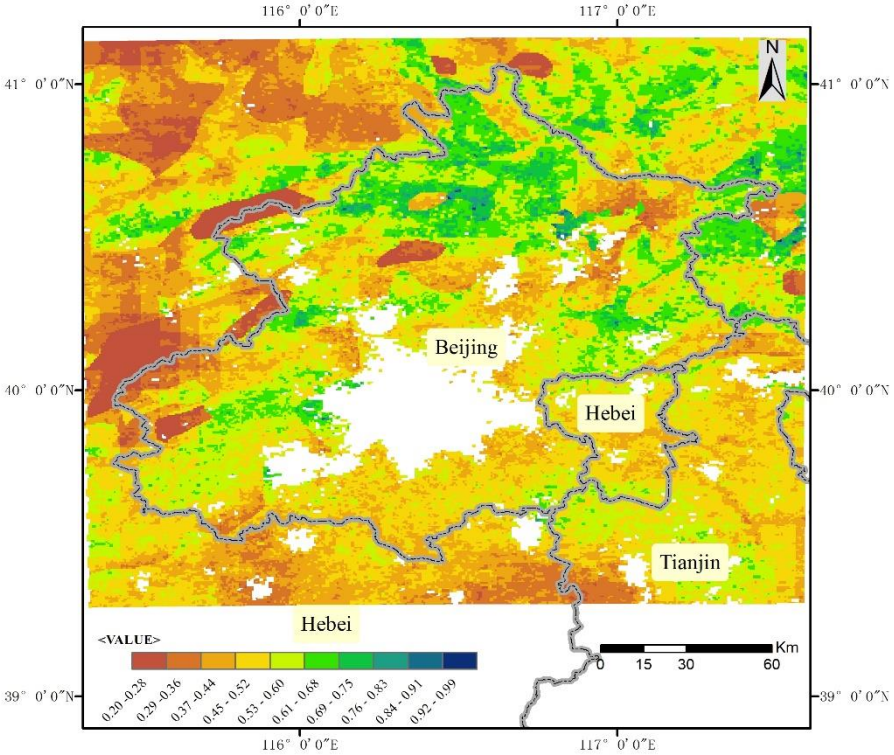

Figure 3.b. Estimated Ω_v spatial distribution (20130901)

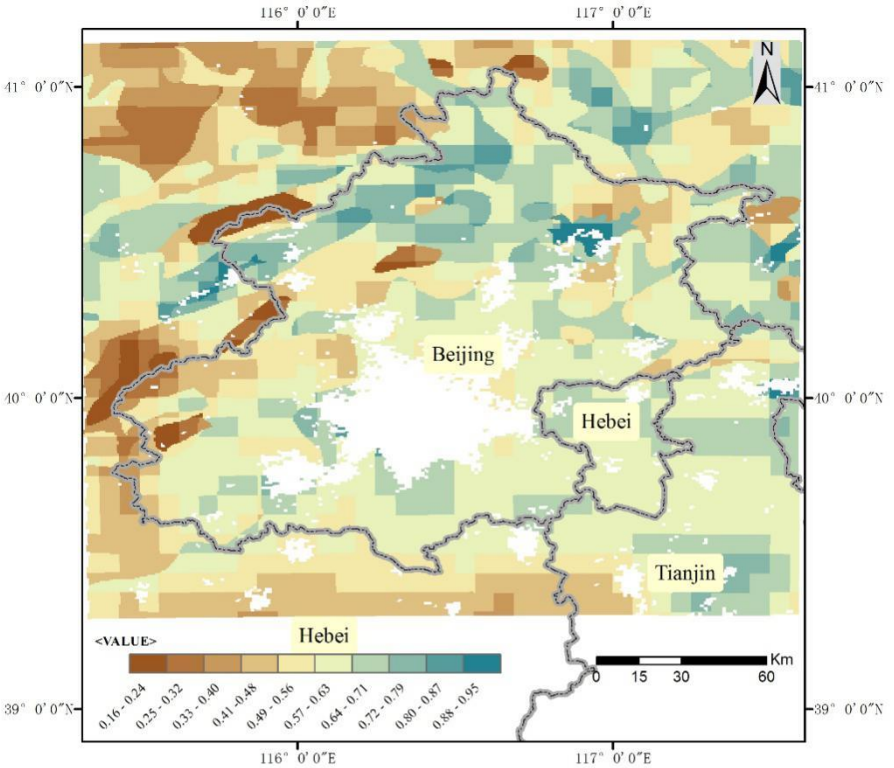

Figure 3. c. Estimated Ω_s spatial distribution (20130901)

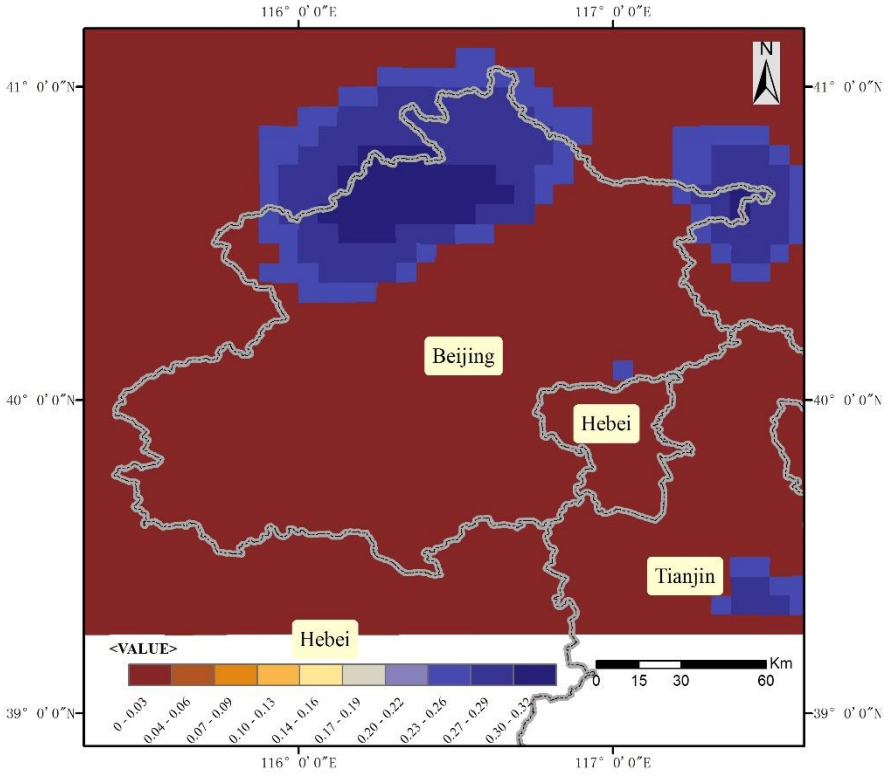

Figure 3. d. Estimated f_{wet} spatial distribution (20130901)

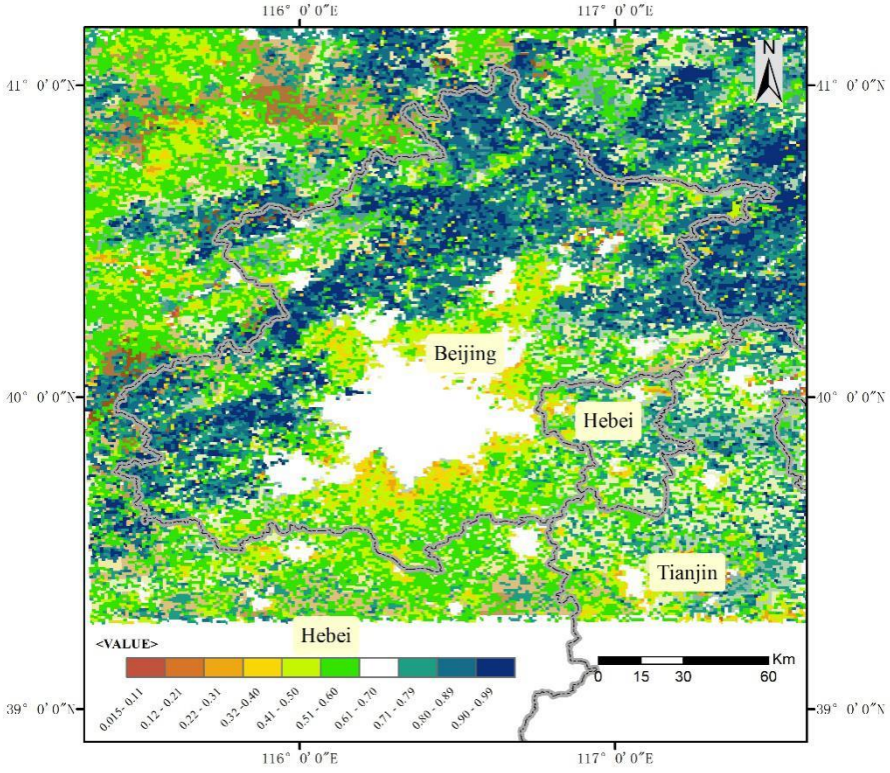

Figure 3.e. Estimated f_c spatial distribution (20130901)

Regional ET_p is estiamted based on PM model, reanalysis datasets and net radiation and ground fluxes estimation results. ET_p range from 1.50 mm d^{-1} to 11.59

mm d^{-1} with the mean value of 3.17 mm d^{-1}. The high ET_p values distribute in the northeast and southwest part of study area and the ET_p values exceed 6.4 mm d^{-1}. The low ET_p value distribute in the southeast part of study area, and the ET_p values are lower than 3.51 mm d^{-1}.

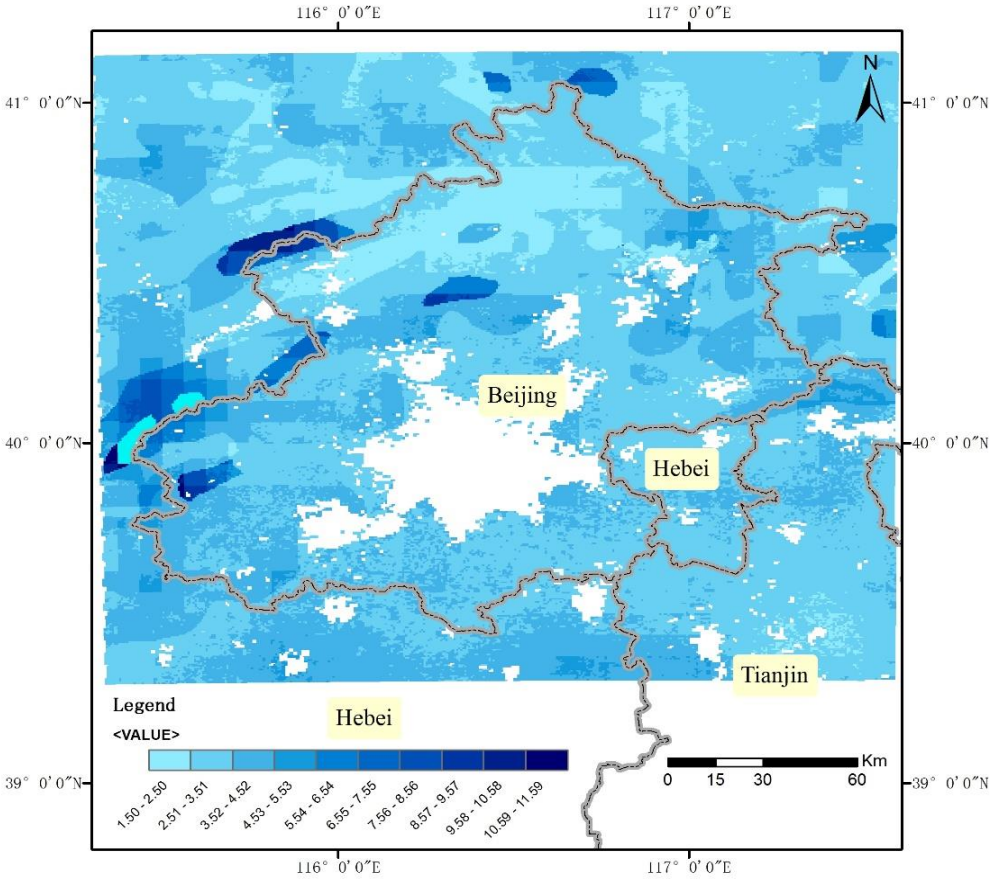

Figure 4. Estimated ET_p spatial distribution (20130901, mm d^{-1})

Regional ET_a is estiamted based on reginal Ω and ET_p estimation results. ET_a ranges from 0.24 mm d^{-1} to 3.87 mm d^{-1} with the mean value of 1.51 mm d^{-1} In the northwest region, due to high ET_p value and low Ω value, ET_a is low with the value ranged from 0.24 mm d^{-1} to 1.69 mm d^{-1}. In the southeast region, due to low ET_p value and low Ω value, ET_a is also low with the values range from 1.34 mm d^{-1} to 2.05 mm d^{-1}.The high ET_a values distribute in the northeast, southwest and central region due to high Ω and high ET_p, with the ET_a ranges from 2.06 mm d^{-1} to 3.15 mm d^{-1}. The regions with high ET_a values agree well with the regions with high soil moisture and air humidity area.

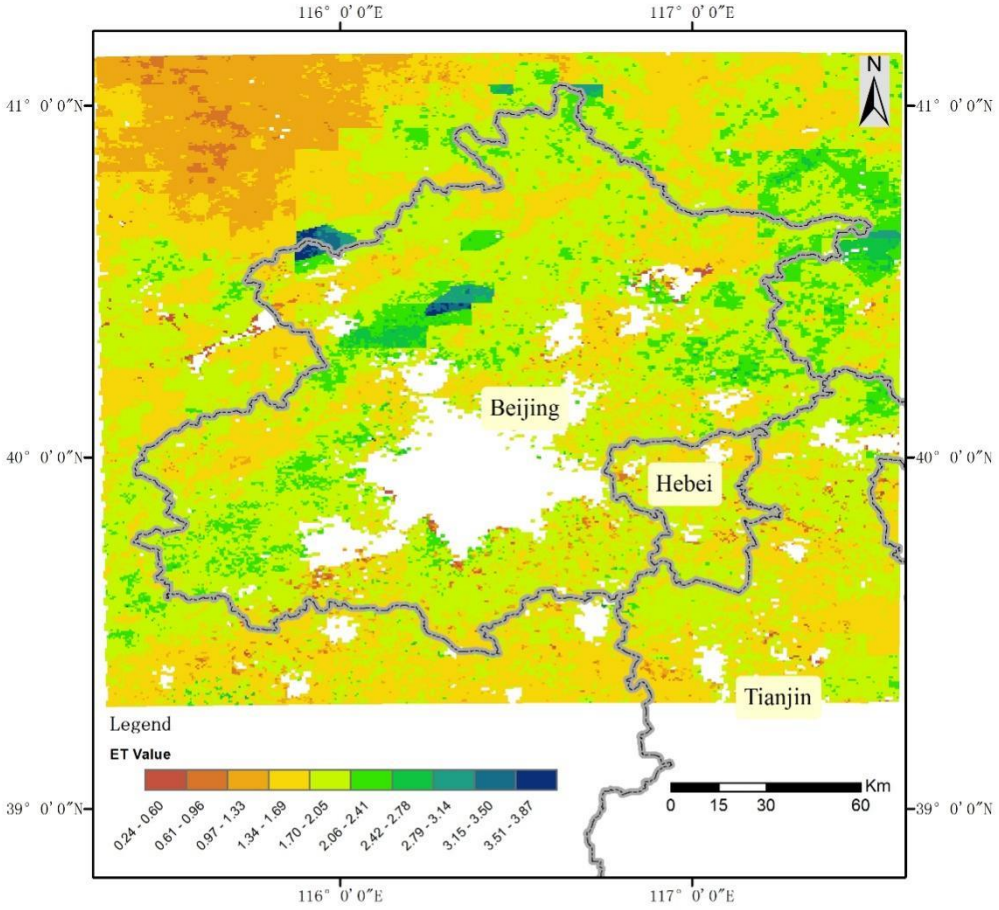

Figure 5. Estimated ET_a spatial distribution (20130901, mm d^{-1})

4.1.2 Regional ET calculation results for the growing season

The decouple model is applied to produce ET products in study area and the calculation period is from 1st, May to 31th, October which is the main vegetation growing season in the years from 2013 to 2020. The estimated ET datasets include 1472 daily regional ET results. Based on the results, the ET change patterns of different underlying surfaces is analyzed, and the high water consumption period and high water consumption area is found and it provides important support for the efficient utilization of water resources in the study area.

Taking 2013 as an example, the daily ET results are cumulative to obtain the total water consumption throughout the growing season. The total regional water consumption is 215~597 mm. The regions with high water consumption values area are mainly located in northeast, southwest and central parts, the total water consumption exceeds 400 mm. Followed by the southeast plain farmland area, the total water

consumption is about 330~400 mm. again for the suburban area of the city is 290~330 mm, The area with the least water consumption is located in the northwest of the study area and cumulative ET is less than 260 mm. Over vegetated surfaces, the total water consumption was generally above 400 mm, which agreed well with the results from Zheng et al. (2020) who reported the multi-year average ET from MOD16 from 2005 to 2015 in Beijing was about 406.63 mm.

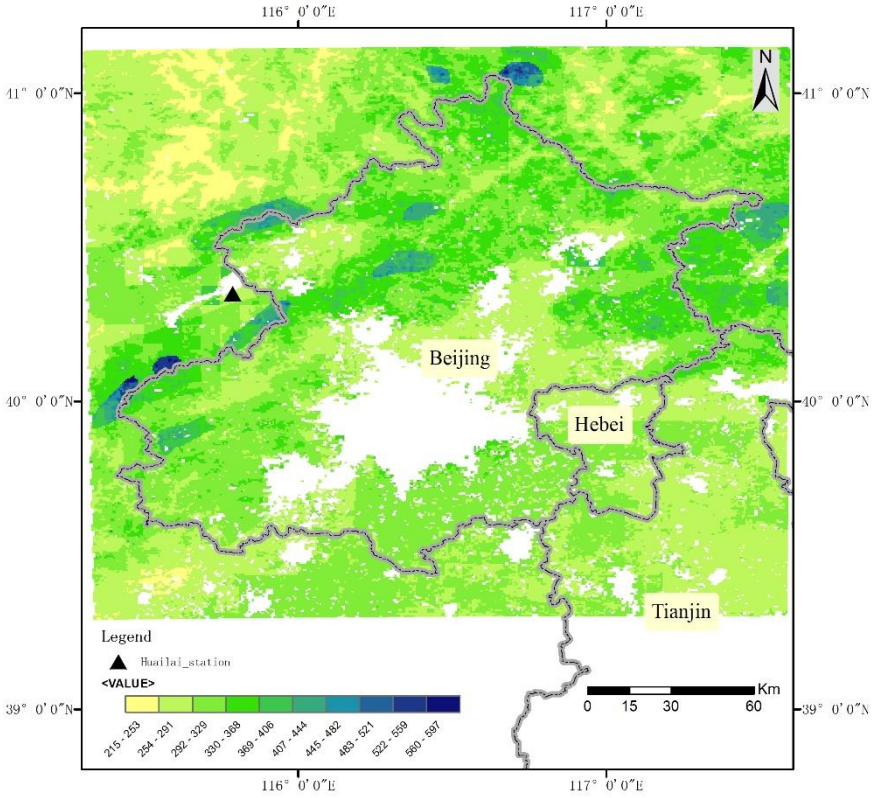

Figure 6. Spatial distribution pattern of total water consumption (mm) in the growing season in the study area

4.1.3 Comparisons with field-measured data for the vegetation growing season

In this study, the inversed ET results from 1st, May, 2013 to 31th, October, 2020 are extracted and compared with the long-term series ET data measured at Huailai Station. The long-term estimated ET series and measured ET series are shown in Figure7. The measured daily ET value is 0.09 ~ 3.48 mm d^{-1}, and the estimated daily ET value is 0.17 ~ 3.02 mm d^{-1}. The increasing and decreasing trends of estimated ET and measured ET is basically consistent while differences exist in daily ET, in which measured ET is generally observed larger than estimated ET, and the largest difference between estimated ET and measured ET was observed in October, 2014, while the smallest difference is observed in September, 2014. Taking 2013 as an example, the

highest regional avrage monthly ET is 69 mm in July with the minimum value of 31.87mm and the maximum value of 130.97mm. The lowest regional average monthly ET is 28.66 mm in October, with the minimum value of 20.43mm and the maximum value of 52.51 mm. In 2013, the sum of the inversed daily ET is 276 mm, the sum of the measured day ET is 234 mm and the accuracy is 85%.

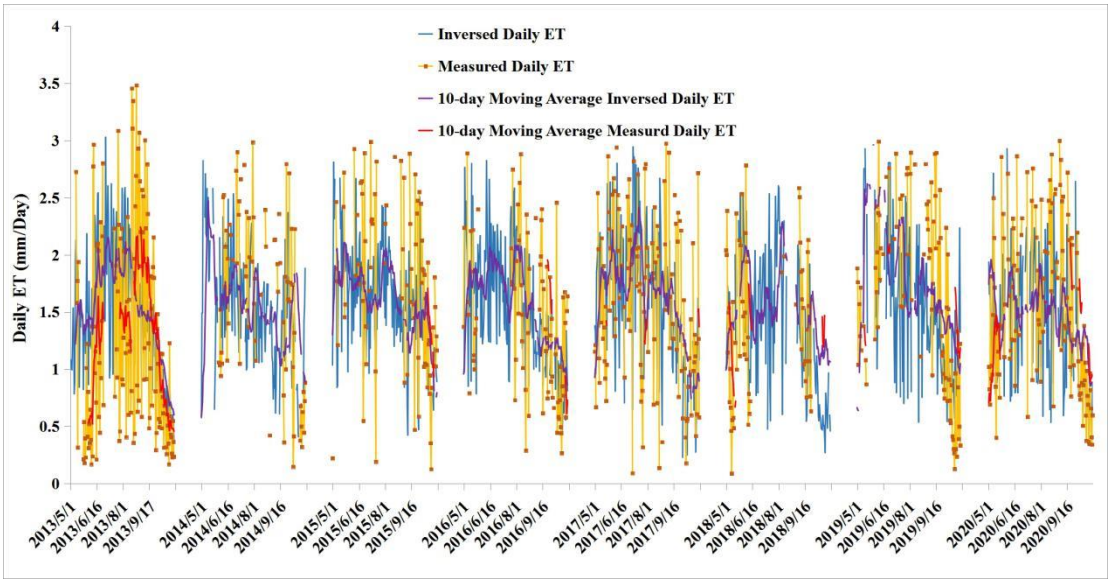

Figure 7. Time series plot for inversed daily ET values and measured ET values at Huailai station from 1st, May, 2013 to 31th, October, 2020 in vegetation growing seasons.

The mean value of the daily estimated ET value from 1st, May, 2013 to 31th, October, 2020 is 1.40 mm d^{-1} and the mean value of the daily measured ET is 1.52 mm d^{-1}. The bias value is -0.12 mm d^{-1}, the RSME average value is 0.66 mm d^{-1}, and the correlation coefficient is 0.52. Therefore, the results of the Decouple method are with high accuracy throughout the vegetation growing season compared with measured ET values.

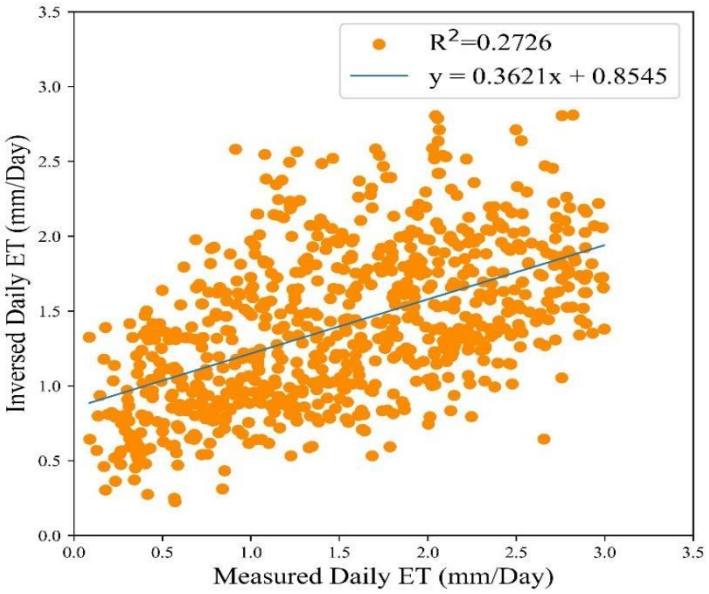

Figure 8. Comparison between inversed daily ET values and measured ET values at Huailai stations from 1st, May, 2013 to 31th, October, 2020

To better illustrate the accuracy of the inversed ET from 1st, May, 2013 to 31th, October, 2020 at Huailai Station, the differences of the accuracy of the estimated ET and the in-situ observations on clear and cloudy days are compared (Figure 9). Besides, the differences over three crop growing stages which include biomass increasing stage (May and June), biomass peak stage (July and August) and biomass decreasing stage (September and October) are also compared (Figure 10). The accuracy on clear days is better than that on cloudy days. Note that the number of days in 8 years is 1472 theoretically, whereas the observed LE is only valid for 784 days, with 498 of clear days and 286 for cloudy days. Specifically, on clear days, the bias is -0.13 mm d^{-1}, the RSME is 0.66 mm d^{-1}, and the correlation coefficient is 0.53, while on cloudy days, the bias is -0.11 mm d^{-1}, the RSME is 0.69 mm d^{-1}, and the correlation coefficient is 0.50. There are no significant differences between the results on clear and cloudy days. Additionally, over three crop growing stages, the estimated result in biomass decreasing stage is the best, which may be attributed to the relatively stable underlying surface and weather conditions. Concretely, the bias is 0.05 mm d^{-1}, -0.17 mm d^{-1} and -0.19 mm d^{-1} over three crop growing stages, respectively, the RSME is 0.66 mm d^{-1}, 0.75 mm d^{-1} and 0.60 mm d^{-1} over three crop growing stages, respectively, the correlation coefficient is 0.47, 0.35 and 0.61 over three crop growing stages, respectively.

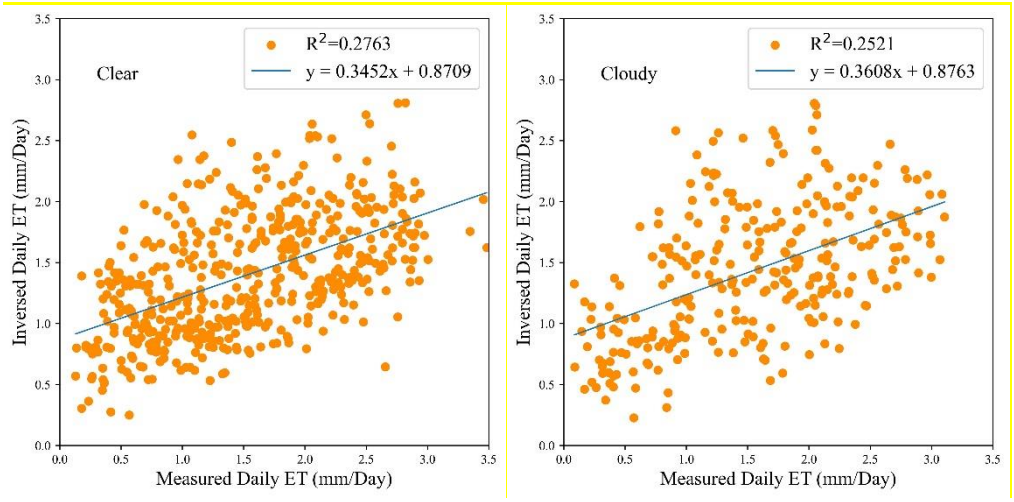

Figure 9. Comparison between inversed daily ET values and measured ET values at Huailai stations from 1st, May, 2013 to 31th, October, 2020 on clear and cloudy days

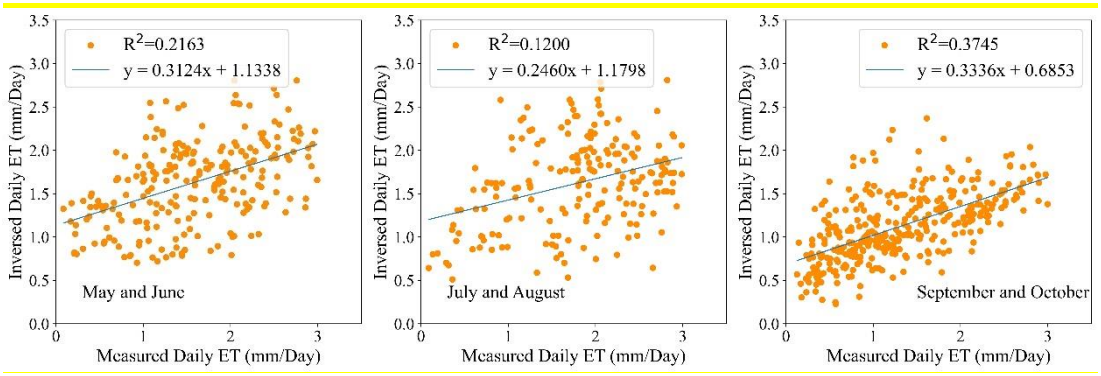

Figure 10. Comparison between inversed daily ET values and measured ET values at Huailai stations from 1st, May, 2013 to 31th, October, 2020 over three crop growing stages

Apart from that, to better interpret the trend of the inversed ET, the ET results from 6th, May to 6th, October, 2013 are extracted and compared with the estimate the reference ET (ET_0) in Badaling Forest Farm. The inversed ET series and estimated ET_0 series are shown in Figure 11. The trends of the inversed ET and the estimated ET_0 are basically akin, whereas ET_0 is generally larger than ET. Besides, the maximum ET_0 is observed on 28th, July, 2013 with the value of 4.06 mm d^{-1}, while the maximum estimated ET is observed on 2nd, July, 2013 with the value of 3.03 mm d^{-1}.

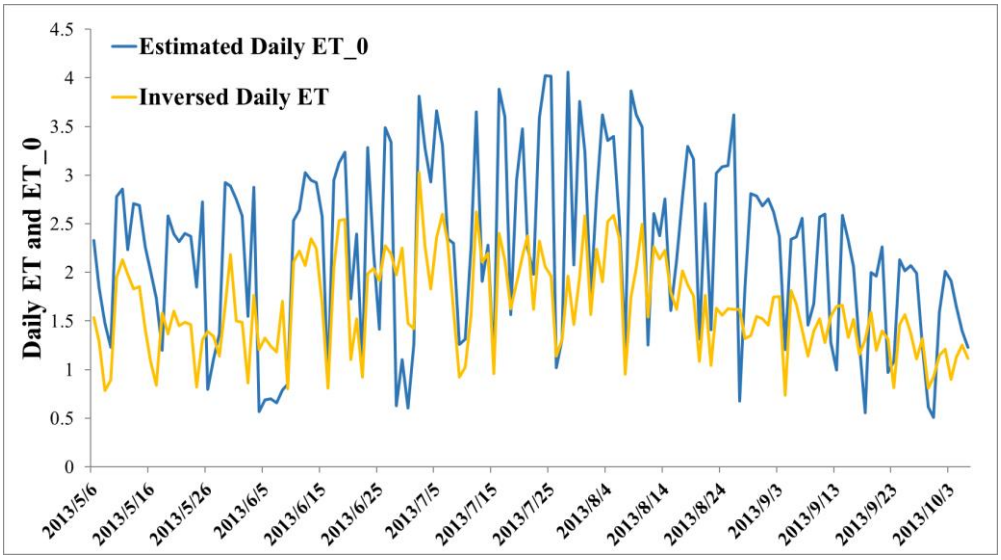

Figure 11. Time series plot for inverted daily ET values and estimated ET_0 values in Badaling Forest Farm from 6th, May to 6th, October in 2013.

Besides, ET_0 was translated into ET using the PM equation combined with crop coefficients. The mean value of the daily inversed ET value from 6th, May to 6th, October, 2013 is 1.64 mm d^{-1} and the mean value of the estimated ET from ET_0 is 1.90 mm d^{-1}. The bias value is 0.26 mm d^{-1}, the RSME average value is 0.74 mm d^{-1}, and the correlation coefficient is 0.73. Therefore, the results of the Decouple method are with high accuracy throughout the vegetation growing season compared with estimated ET and ET_0 values using PM equation.

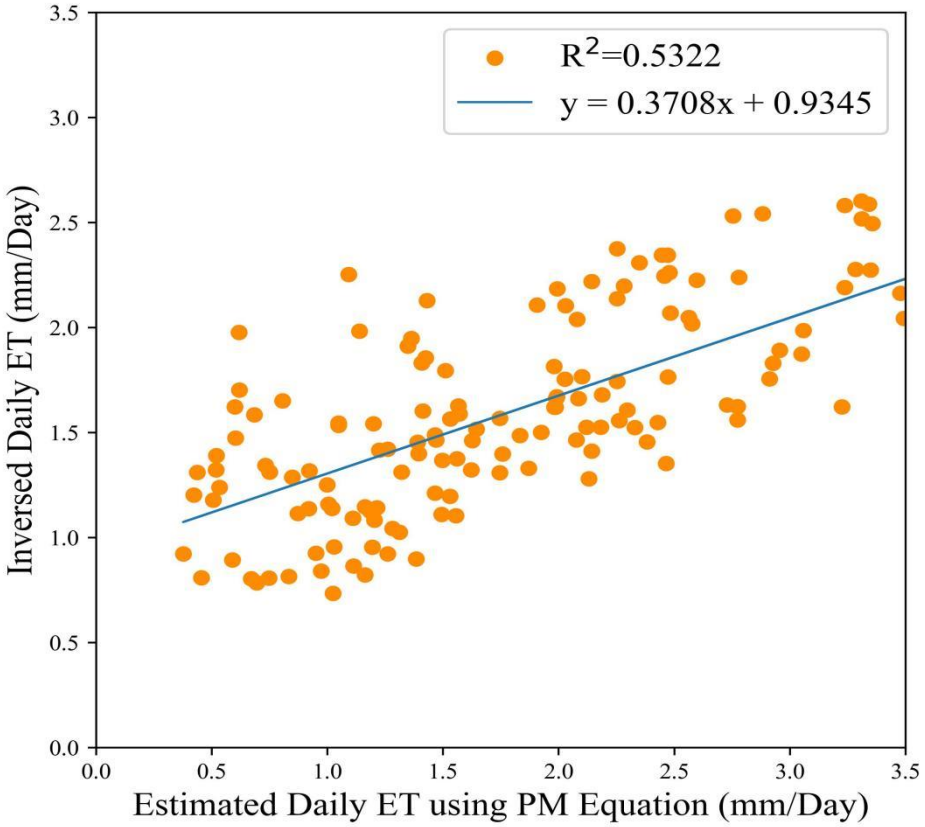

Figure 12. Comparison between inverted daily ET values and estimated ET values using PM equation in Badaling Forest Farm from 6th, May to 6th, October, 2013

4.2 Regional water consumption quantity and water-consuming patterns for different ecosystems

4.2.1 Seasonal variation of vegetation water consumption in the study area

In the study area, the total water consumption in the vegetation growing season which was from 1st, May to 31th, October in 2013 is 4.203 billion m^3. The largest water consumption month is July, and the total water consumption is 0.92 billion m^3, accounting for about 22% of the total water consumption, mainly due to the highest air temperature in that month, the strongest downward radiation, the largest available soil moisture. The regional average monthly ET is 69 mm in July, and it is followed by August, June, May and September, with 0.84 billion m^3, 0.77 billion m^3, 0.75 billion m^3, 0.54 billion m^3, respectively. The total water consumption in October is the smallest, with a total water consumption of 0.37 billion m^3, accounting for 9% of the total water consumption.

Table 1. Quantity of water consumed by vegetation in different seasons from 1st, May to 31th, October in 2013

Month	**Minimum ET （mm）**	**Maximum ET （mm）**	**Average ET （mm）**	**Regional water consumption (*10^9 m^3)**
May	21.15	174.90	54.43	0.75
Jun.	25.90	115.83	57.07	0.77
Jul.	31.87	130.97	69.00	0.92
Aug.	36.61	143.39	63.75	0.84
Sep.	25.24	81.15	41.66	0.54
Oct.	20.43	52.51	28.66	0.37
Sum				4.20

4.2.2 Water-consuming patterns for different ecosystems

The total water consumption is accumulated and analyzed by overlaying the vegetation types distribution layer on the ET results layers to obtain the total annual water consumption of different vegetation types in 2013, as shown in Figure 14. The largest total water consumption is temperate deciduous broad-leaved forest, with a total annual water consumption of 427 mm, followed by mixed forest, evergreen coniferous forest, deciduous shrubland, deciduous small-leaved forest, annual double croping farmland, annual double croping farmland with the ET values of 412 mm, 369 mm, 314 mm, 290 mm, 290 mm 289 mm, respectively. Temperate steppe consumps the lowest water with a total ET of 276 mm. The results of total water consumption over different vegetation types are consitent with the results of Zheng et al. (2020) who also reported that the largest total water consumption is in forests and the lowest total water consumption is in grasslands among forests, farmlands and grasslands.

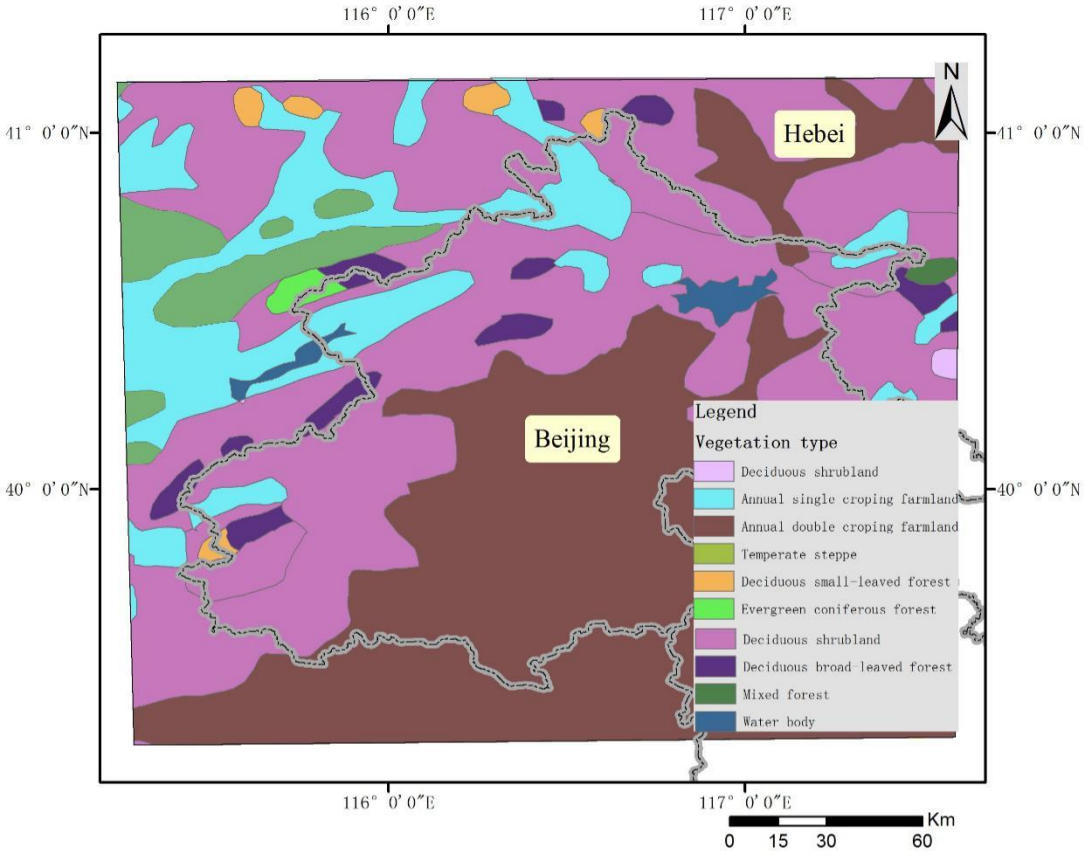

Figure 13. Spatial distribution of the main vegetation types in the study area

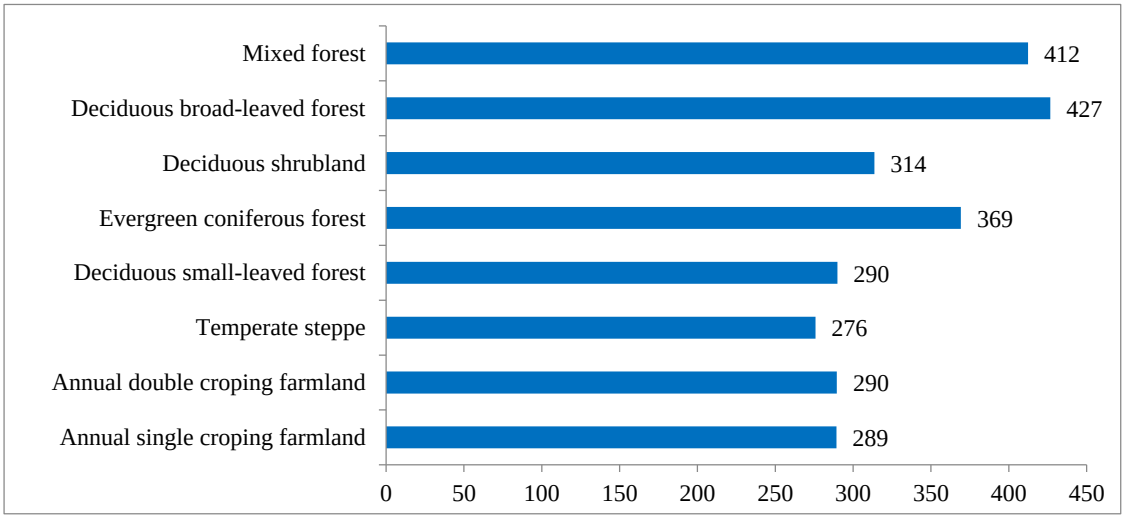

Figure14. Statistical results of water consumption of different types of vegetation in the study area (mm)

5. Summary and conclusion

In this study, a parameterization method for decouple model is developed and applied to inverse regional ET in Beijing City and nearby region from 2013 to 2020 in a case study, using MODIS remote sensing data, CLDAS reanalysis data, and basic

geography information data. The inversed ET results are compared with the measured ET values at Huailai station, showing that the inversed ET values ranged from 0.17 mm d^{-1} to 3.02 mm d^{-1}. In contrast, the measured ET values range from 0.09 mm d^{-1} to 3.48 mm d^{-1}. Besides, comparing to the sum of the measured daily ET in 2013 of 234 mm, the sum of the inversed daily ET is 276 mm with the accuracy of 85%. Specifically, daily ET range from 0.24 mm d^{-1} to 3.87 mm d^{-1} with the mean value of 1.51 mm d^{-1} on 1st, September 2013, and the regions with high ET values agree well with the regions with high soil moisture and air humidity area. These results show that the decouple model is with great potential to generate regional daily ET products.

Based on the ET estimation results, the spatiotemporal variation law of water consumption in Beijing is deeply analyzed. Chronologically, the high water consumption period is from June to August with the largest water consumption in July of 2013 with the value of 0.92 billion m^3, accounting for about 22% of the total water consumption. Further, the ecosystem with the highest water consumption is temperate deciduous forest, with the value of 427 mm, followed by mixed forest, temperate evergreen coniferous forest, temperate deciduous shrubland, deciduous small-leaved forest, crop and fruit tree, and temperate grassland, which provides an important reference for monitoring the regional water resource use efficiency.

However, the inversed ET results from the decouple method is influenced by such factors as remote sensing data (spatial resolution of 500 m) of vegetation index, reflectance, etc., and reanalysis datasets (spatial resolution of 0.0625°) of air temperature, solar radiation, etc.. Besides, the overall spatial resolution is relatively coarse, thereby it can only analyze the trend of hydrothermal flux trend and pattern in a large area, rather than the function of describing hydrothermal flux trend and pattern on local small scale. Moreover, the spatial resolutions of remote sensing products, reanalysis products and basic geography information are uneven, which also brings certain uncertainty to the inversion results. In addition, there are gaps in the vegetation coverage of MODIS in urban areas and water bodies, resulting in gaps in the production of ET products in these areas. Integrating higher resolution vegetation index and

reflectivity products as well as land use and land cover datasets is necessary to solve this problem.

Further, limited by the collected data, ET inversion studies were only carried out within 1472 days in vegetation growing season in 8 years in Beijing City and nearby region, and the measured data applied to validation was only at two site. In the future, on one hand, it is necessary to apply this method on a larger regional scale to carry out long-term continuous evapotranspiration inversion research. On the other hand, the current conclusions were only based on the Huailai station, more representative sites are needed to collect measured flux, meteorological factors in multiple ecosystems and climatic zone conditions, to validate the ET inversion results, analyze the spatiotemporal trend of water consumption in study area and to support irrigation management, so as to lay a foundation for the further promotion of this method.

Acknowledgement

This work was supported in part by the Beijing Natural Science Foundation under Grant 8184075, and in part by the Beijing Municipal Science and Technology Project (NO. Z181100005318003) and Ministry of Water Resources Young Top Talents Program (2022).

References

Allen, R. G., L. S. Pereira, D. Raes, and M. Smith. 1998. Crop evapotranspiration: guidelines for computing crop water requirements - FAO irrigation and drainage paper 56 [EB/OL]. http://www.fao.org/docrep/X0490E/x0490e06.htm

Bastiaanssen, W. G. M. 2000. “SEBAL-based sensible and latent heat fluxes in the irrigated Gediz Basin, Turkey.” *Journal of Hydrology* 229(1–2):87–100.

Boegh, E., H. Soegaard, and A. Thomsen. 2002. “Evaluating evapotranspiration rates and surface conditions using Landsat TM to estimate atmospheric resistance and surface resistance.” *Remote Sensing of Environment* 79(2–3):329–343.

Caparrini, F., F. Castelli, and D. Entekhabi. 2004. “Variational estimation of soil and vegetation turbulent transfer and heat flux parameters from sequences of multisensor imagery.” *Water Resources Research* 40(12):1–15.

Crosson, W. L., M. Z. Al-Hamdan, S. N. J. Hemmings, and G. M. Wade. 2012. “A daily merged MODIS Aqua-Terra land surface temperature data set for the conterminous United States.” *Remote Sensing of Environment* 119:315–324.

Di, S. C., Z. L. Li, R. Tang, H. Wu, B. H. Tang, and J. Lu. 2015. “Integrating two layers of soil moisture parameters into the MOD16 algorithm to improve evapotranspiration estimations.” *International Journal of Remote Sensing* 36(19–20):4953–4971.

Duan, S. B., Z. L. Li, and P. Leng. 2017. “A framework for the retrieval of all-weather land surface temperature at a high spatial resolution from polar-orbiting thermal infrared and passive microwave data.” *Remote Sensing of Environment* 195:107–117.

Fisher, J. B., K. P. Tu, and D. D. Baldocchi. 2008. “Global estimates of the land-atmosphere water flux based on monthly AVHRR and ISLSCP-II data, validated at 16 FLUXNET sites.” *Remote Sensing of Environment* 112(3):901–919.

Goldberg, V., and C. Bernhofer. 2001. “Quantifying the coupling degree between land surface and the atmospheric boundary layer with the coupled vegetation-atmosphere model HIRVAC.” *Annales Geophysicae* 19(5):581–587.

Granata, F. 2019. “Evapotranspiration evaluation models based on machine learning algorithms—A comparative study.” *Agricultural Water Management* 217(January):303–315.

Jackson, R. D., W. P. Kustas, and B. J. Choudhury. 1988. “A reexamination of the crop water stress index.” *Irrigation Science* 9(4):309–317.

Jackson, R. D., R. J. Reginato, and S. B. Idso. 1977. “Wheat canopy temperature: A practical tool for evaluating water requirements.” *Water Resources Research* 13(3):651–656.

Jung, M., M. Reichstein, P. Ciais, S. I. Seneviratne, J. Sheffield, M. L. Goulden, G. Bonan, … K. Zhang. 2010. “Recent decline in the global land evapotranspiration trend due to limited moisture supply.” *Nature* 467(7318):951–954.

Kang, L., J. Zhang, X. Zou, H. Cheng, C. Zhang, and Z. Yang. 2019. “Experimental Investigation of the Aerodynamic Roughness Length for Flexible Plants.” *Boundary-Layer Meteorology* 172(3):397–416.

Kool, D., N. Agam, N. Lazarovitch, J. L. Heitman, T. J. Sauer, and A. Ben-Gal. 2014. “A review of approaches for evapotranspiration partitioning.” *Agricultural and Forest Meteorology* 184:56–70.

Kustas, W. P., and K. S. Humes. 1995. “Source approach for estimating soil and vegetation energy fluxes in observations of directional radiometric surface temperature.” *Agricultural and Forest Meteorology* 77(3–4):263–293.

Kustas, W. P., X. Zhan, and T. J. Schmugge. 1998. “Combining optical and microwave remote sensing for mapping energy fluxes in a semiarid watershed.” *Remote Sensing of Environment* 64(2):116–131.

Li, Z. L., R. Tang, Z. Wan, Y. Bi, C. Zhou, B. Tang, G. Yan, and X. Zhang. 2009. “A review of current methodologies for regional Evapotranspiration estimation from remotely sensed data.” *Sensors* 9(5):3801–3853.

Long, D., B. R. Scanlon, L. Longuevergne, A. Y. Sun, D. N. Fernando, and H. Save. 2013. “GRACE satellite monitoring of large depletion in water storage in response to the 2011 drought in Texas.” *Geophysical Research Letters* 40(13):3395–3401.

Ma, J., H. Shen, P. Wu, J. Wu, M. Gao, and C. Meng. 2022. “Generating gapless land surface temperature with a high spatio-temporal resolution by fusing multi-source satellite-observed and model-simulated data.” *Remote Sensing of Environment* 278(April).

McNaughton, K. G., and P. G. Jarvis. 1983. *Predicting Effects of Vegetation Changes on Transpiration and Evaporation*. *Additional Woody Crop Plants*. Vol. VII. ACADEMIC PRESS, INC.

Menenti, M., and B. J. Choudhury. 1993. “Parameterization of land surface evapotranspiration using a location dependent potential evapotranspiration and surface temperature range.” *Exchange processes at the land surface for a range of space and time scales* 212:561–568.

Monteith J. 1965. “Evaporation and Environment.” *Symposia of the society for experimental biology* 19:205–234.

Mu, Q., H. F. Ann, M. Zhao, and Running Steven W. 2007. “Development of a Global Evapotranspiration Algorithm Based on MODIS and Global Meteorology Data.” *Remote Sensing of Environment* 114(4):519–536.

Mu, Q., M. Zhao, and S. W. Running. 2011. “Improvements to a MODIS global terrestrial evapotranspiration algorithm.” *Remote Sensing of Environment* 115(8):1781–1800.

Penman, H. L. 1948. “Natural Evaporation From Open Water, Bare Soil and Grass.” *Proceedings of the Royal Society of London. Series a. Mathematical and Physical Sciences* 193(1032):120–145.

Ramoelo, A., N. Majozi, R. Mathieu, N. Jovanovic, A. Nickless, and S. Dzikiti. 2014. “Validation of global evapotranspiration product (MOD16) using flux tower data in the African savanna, South Africa.” *Remote Sensing* 6(8):7406–7423.

Rana, G., N. Katerji, M. Mastrorilli, and M. El Moujabber. 1997. “A model for predicting actual evapotranspiration under soil water stress in a mediterranean region.” *Theoretical and Applied Climatology* 56(1–2):45–55.

Reichle, R. H., D. B. McLaughlin, and D. Entekhabi. 2002. “Hydrologic data assimilation with the ensemble Kalman filter.” *Monthly Weather Review* 130(1):103–114.

Su, Z. 2002. “The Surface Energy Balance System (SEBS) for estimation of turbulent heat fluxes.” *Hydrology and Earth System Sciences* 6(1):85–99.

Tang, Ronglin., and Z. Li. 2017. “An End-Member-Based Two-Source Approach for Estimating Land Surface Evapotranspiration From Remote Sensing Data.” *IEEE Transactions on Geoscience and Remote Sensing* 55(10):5818–5832.

Tang, Ronglin, and Z. L. Li. 2017. “Estimating Daily Evapotranspiration From Remotely Sensed Instantaneous Observations With Simplified Derivations of a Theoretical Model.” *Journal of Geophysical Research: Atmospheres* 122(19):10177–10190.

Tang, R., Z. L. Li, K. S. Chen, Y. Jia, C. Li, and X. Sun. 2013. “Spatial-scale effect on the SEBAL model for evapotranspiration estimation using remote sensing data.” *Agricultural and Forest Meteorology* 174–175:28–42.

Tang, R., Z. L. Li, and B. Tang. 2010. “An application of the Ts-VI triangle method with enhanced edges determination for evapotranspiration estimation from MODIS data in arid and semi-arid regions: Implementation and validation.” *Remote Sensing of Environment* 114(3):540–551.

Tian, X., Z. Y. Li, C. van der Tol, Z. Su, X. Li, Q. S. He, Y. F. Bao, E. X. Chen, and L. H. Li. 2011. “Estimating zero-plane displacement height and aerodynamic roughness length using synthesis of LiDAR and SPOT-5 data.” *Remote Sensing of Environment* 115(9):2330–2341.

Wang, K., and R. E. Dickinson. 2012. “A review of global terrestrial evapotranspiration: Observation, modeling, climatology, and climatic variability.” *Reviews of Geophysics* 50(2).

Wang, K., P. Wang, Z. Li, M. Cribb, and M. Sparrow. 2007. “A simple method to estimate actual evapotranspiration from a combination of net radiation, vegetation index, and temperature.” *Journal of Geophysical Research Atmospheres* 112(15):1–14.

Wu, P., Y. Su, S. bo Duan, X. Li, H. Yang, C. Zeng, X. Ma, Y. Wu, and H. Shen. 2022. “A two-step deep learning framework for mapping gapless all-weather land surface temperature using thermal infrared and passive microwave data.” *Remote Sensing of Environment* 277(October 2021):113070.

Yang, Y. 2014. “A new remotely sensed model to retrieve regional evapotranspiration considering advection effects.”

Yuan, X., R. Hamdi, F. U. Ochege, P. De Maeyer, A. Kurban, and X. Chen. 2021. “Assessment of surface roughness and fractional vegetation coverage in the

CoLM for modeling regional land surface temperature." *Agricultural and Forest Meteorology* 303(March):108390.

Zhang, K., J. S. Kimball, and S. W. Running. 2016. "A review of remote sensing based actual evapotranspiration estimation." *Wiley Interdisciplinary Reviews: Water* 3(6):834–853.

Zhao, L., J. Xia, C. yu Xu, Z. Wang, L. Sobkowiak, and C. Long. 2013. "Evapotranspiration estimation methods in hydrological models." *Journal of Geographical Sciences* 23(2):359–369.

Zheng, R., M. Cheng, and H. Zhang. 2020. "Impact of Land use Change on Evapotranspiration in Beijing from 2005 to 2015." *Water Resources and Power* 38(2):22–25.